AIP | The Journal of Chemical Physics

Coherent control of the isomerization of retinal in bacteriorhodopsin in the high intensity regime

Valentyn I. Prokhorenko, Alexei Halpin, Philip J. M. Johnson, R. J. Dwayne Miller, and Leonid S. Brown

Citation: The Journal of Chemical Physics **134**, 085105 (2011); doi: 10.1063/1.3554743
View online: http://dx.doi.org/10.1063/1.3554743
View Table of Contents: http://scitation.aip.org/content/aip/journal/jcp/134/8?ver=pdfcov
Published by the AIP Publishing

Coherent control of the isomerization of retinal in bacteriorhodopsin in the high intensity regime

Valentyn I. Prokhorenko,[1,a)] Alexei Halpin,[1] Philip J. M. Johnson,[1] R. J. Dwayne Miller,[1,b)] and Leonid S. Brown[2]

[1]*Max Planck Research Group for Structural Dynamics, Department of Physics, University of Hamburg, Center for Free Electron Laser Science, DESY, Notkestr. 85, 22607 Hamburg, Germany and Departments of Physics and Chemistry, and the Institute for Optical Sciences, University of Toronto, 80 St. George St., Toronto, Ontario M5S 3H6, Canada*

[2]*Department of Physics, University of Guelph, Guelph, Ontario N1G 2W1, Canada*

(Received 19 November 2010; accepted 20 January 2011; published online 23 February 2011)

Coherent control protocols provide a direct experimental determination of the relative importance of quantum interference or phase relationships of coupled states along a selected pathway. These effects are most readily observed in the high intensity regime where the field amplitude is sufficient to overcome decoherence effects. The coherent response of retinal photoisomerization in bacteriorhodopsin to the phase of the photoexcitation pulses was examined at fluences of $10^{15} - 2.5 \times 10^{16}$ photons per square centimeter, comparable to or higher than the saturation excitation level of the $S_0 - S_1$ retinal electronic transition. At moderate excitation levels of $\sim 6 \times 10^{15}$ photons/cm^2 ($<$100 GW/cm^2), chirping the excitation pulses increases the all-*trans* to 13-*cis* isomerization yield by up to 16% relative to transform limited pulses. The reported results extend previous weak-field studies [Prokhorenko *et al.*, Science **313**, 1257 (2006)] and further illustrate that quantum coherence effects persist along the reaction coordinate in strong fields even for systems as complex as biological molecules. However, for higher excitation levels of $\sim$200 GW/cm^2, there is a dramatic change in photophysics that leads to multiphoton generated photoproducts unrelated to the target isomerization reaction channel and drastically changes the observed isomerization kinetics that appears, in particular, as a red shift of the transient spectra. These results explain the apparent contradictions of the work by Florean *et al.* [Proc. Natl. Acad. Sci. U.S.A. **106**, 10896 (2009)] in the high intensity regime. We are able to show that the difference in observations and interpretation is due to artifacts associated with additional multiphoton-induced photoproducts. At the proper monitoring wavelengths, coherent control in the high intensity regime is clearly observable. The present work highlights the importance of conducting coherent control experiments in the low intensity regime to access information on quantum interference effects along specific reaction coordinates. © *2011 American Institute of Physics*. [doi:10.1063/1.3554743]

I. INTRODUCTION

Quantum coherence effects in the light–matter interaction can affect the populations of quantum states or the outcome of a photochemical reaction. These effects can be explored using the coherent control protocol where excitation light pulses with specifically tailored temporal shapes trigger different quantum pathways whose constructive or destructive interference can enhance or suppress an observable of interest (e.g., the amount of desired isomer in a photoisomerization reaction). In coherent control, the spectral modulation of excitation pulses sets the different components of the wave packets in the ground and excited state potential surfaces, while phase modulation sets their relative phases, allowing control of wave packet propagation and focusing. Experiments with only phase modulation can provide the most direct information about the phase sensitivity of the field–matter interaction and is frequently called "pure" coherent control. In such experiments, the overlap between the sample absorption spectrum and the laser spectrum remains unchanged upon phase modulation.

In the resonant case, nondestructive coherent control can be generally divided into weak-field and strong-field regimes. In the weak-field limit, the light fluence (or its intensity) is lower by many orders of magnitude than the characteristic nonlinear threshold given by the saturation fluence (intensity) of the relevant optical transitions. Such control can be realized in open quantum systems where the system of interest interacts with an excitation field and with the environment or bath. The first experimental study in this regard was performed in Ref. 1, where an enhancement of the excited state population of a solvated dye was observed for the most general case of amplitude and/or phase shaping under constant actinic conditions. Subsequently, similar experiments were conducted using phase-only control.[2,3] Successful weak-field control of the photochemical reaction, isomerization of the retinal chromophore in the protein bacteriorhodopsin (bR), was demonstrated in Ref. 4. This experimental work confirmed that quantum coherence effects in biological systems can persist

a)Electronic mail: valentyn.prokhorenko@mpsd.cfel.de.
b)Electronic mail: dmiller@lphys.chem.utoronto.ca.

long enough to influence their function; in this case, the primary step in proton translocation.[5] In these investigations, both amplitude and phase modulation of the spectral components of the excitation pulse were employed. The weak-field pure phase control of retinal isomerization in bR was additionally performed in Ref. 6. It was demonstrated that the phase influence contributes only 5%–7% to the overall effect of the all-*trans* to 13-*cis* isomerization control (±20%, Ref. 4). Recent theoretical work has confirmed the ability to control an outcome in open quantum systems using phase shaping in the weak-field limit.[7]

In strong fields the corresponding intensities are much higher and the quantum system interacts many times with the field (multiphoton processes); thus, many pathways will contribute to the formation of a target state by quantum interference. Even closed quantum systems can be controlled in this regime, and even the simplest two-level system populations can be manipulated using pure phase pulse shaping. Experimental strong-field control of the population transfer in organic dyes and biological molecules was demonstrated for the first time in Refs. 8 and 9 using chirped excitation pulses and in Ref. 10 using closed-loop optimization. The effect of population enhancement in strong fields is explained in the framework of the Rice–Tannor "pump-dump" scenario,[11] where the chirping of excitation pulses either prevents the downhill population transfer from excited to ground state (positive chirp, enhancement of excited state population) or accelerates it (negative chirp, suppression of excited state population). In the theoretical work of Fainberg and Gorbunov,[12] the chirp influence on the population transfer was analyzed for open quantum systems beyond the Markov limit with the inclusion of excited state absorption (ESA). The authors found that excitation with transform limited (TL) pulses leads to a minimization of the excited state population and its chirp dependence has a nearly symmetric ν-like shape. According to Ref. 13, for two-level systems with non-Markovian dissipation, the shape of the chirp dependence should have significant asymmetry, with more efficient population transfer for the positively chirped pulses.

The first experimental attempt to control photoisomerization in intense fields was reported recently by Greenfield *et al.*,[14] where the authors investigated the *cis*- to *trans*-stilbene isomerization branching ratio using shaped UV pulses. The authors found that the excitation with TL pulses minimizes the amount of *trans*-stilbene, and the experimentally observed chirp dependence of the branching ratio agrees well with the theoretical prediction.[12]

In contrast to the work of Greenfield *et al.*,[14] Florean *et al.*[15] reported that optimal control of photoisomerization is achieved with TL pulses. The authors investigated all-*trans* to 13-*cis* retinal isomerization in bR at excitation levels up to 1.8×10^{16} photons/cm^2 using a closed-loop optimization protocol and chirp scans. As a target, the authors chose the transient absorption signal measured at 650 nm 40 ps after excitation. In these experiments, they did not detect any sensitivity of the isomerization yield to the pulse shapes for excitations lower than 6×10^{15} photons/cm^2; however, at higher excitations they found that only TL pulses led to an increase in the target signal. From these observations, the authors concluded that in the high intensity regime the TL pulse maximizes the all-*trans* to 13-*cis* retinal isomerization yield in bR and is, thus, the "optimal pulse." They asserted that quantum coherence does not seem to play a significant role in the high intensity regime. This observation is unusual as quantum coherence effects are manifestly larger in the high intensity regime where the effects of decoherence can be overcome by sufficiently intense fields to drive constructive and destructive interference effects. The sensitivity of these experiments was noted to be a limiting factor in the study of the low intensity regime. However, the results in the high intensity regime are contrary to the general trends observed for similarly complex molecules. The basic argument in Ref. 15 was that a new pathway involving a higher lying excited state is a more efficient channel for isomerization than that associated with the first excited state of bR. In this scenario, transform limited pulses were assigned to be the optimal pulse shape for a fixed bandwidth as such pulses have the highest peak power and highest degree of multiphoton absorption to populate these upper level states. These observations are unusual in that all previous studies of coherent control under high intensity conditions have shown a clear chirp dependence that optimizes reaction yields. In addition, this upper level excited state surface would not be accessed under normal biological conditions; yet would have to be more efficient than the evolutionary optimized isomerization process in bR, which is effectively barrierless. This interpretation is interesting and needs to be put in the proper context. The photoactive pigment in bR is retinal. In solution, there are a multitude of photoproducts with only a few percent quantum yields.[16,17] In the protein environment, there is a dominant photoproduct observed, the *cis* C13 = C14 isomer, with a quantum yield of 65%.[18,19] Photoisomerization occurs in competition with the rapid internal conversion process of retinal. All these facts indicate that this photoreaction is highly optimized in the protein environment. The high intensity studies of Florean *et al.*[15] taken at face value suggest otherwise. These observations bear critically on previous coherent control studies in the high intensity regime as well as have significant implications in assessing the degree of evolutionary optimization versus incidental effects of protein structure in directing reaction coordinates. The lack of any clear signature of coherent control in the high intensity regime, where this process should be more efficient, also draws into question earlier studies under weak-field conditions.[4,6]

To resolve this issue, we conducted an investigation of the retinal photoisomerization in bR under similar excitation conditions as in Ref. 15, but in a wide range of excitation fluences and observed over broad spectral and delay ranges with an order of magnitude higher precision. We found that at moderate excitations of $\leq 6 \times 10^{15}$ photons/cm^2 (< 100 GW/cm^2) the all-*trans* to 13-*cis* retinal isomerization in bR can be effectively controlled using chirped pulses and that the TL pulse minimizes the isomerization yield, as expected. However, at higher intensities exceeding 100 GW/cm^2, additional channels including perhaps ionization of the protein come into play and significantly alter the isomerization process. In the

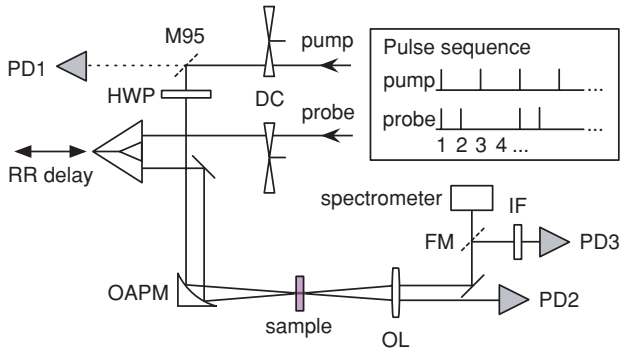

FIG. 1. Optical layout of the pump–probe setup used in the study. M95–95% aluminum mirror, HWP–half-wave plate, RR–hollow retroreflector, OAPM – off-axis parabolic mirror ($f = 15$ cm), OL–collimating objective, FM–flip mirror, IF–interference filter, PD1..3–photodiodes. Inset shows the pulse sequence using dual chopping (DC).

transient absorption, these effects appear as a red shift in the observed differential absorption spectra, indicative of a photoprocess that is unrelated to the reaction coordinate of interest.

II. MATERIALS AND METHODS

A. Experimental setup

The coherent control experiments have been carried out in a pump–probe configuration similar to Ref. 1 (see Fig. 1) with slight modifications: (i) to focus the collimated pump and probe beams into the sample cell we used an off-axis parabolic mirror instead of a spherical mirror, as was the case in previous experiments,[1,4,6] and (ii) an additional photodiode was used to measure the energy of the transmitted pump beam. The off-axis parabolic mirror allows for a tighter focusing of the beams into the sample cell and, thus, a higher energy density therein. The differential absorption spectra were measured under the "magic angle" condition using a spectrometer with a resolution of 1.3 nm in a 200-nm spectral window (Sciencetech, model 9057, 300 mm^{-1} grating, Canada) equipped with a fast photodiode array sensor (S3902, Hamamatsu, Japan). Since the intrinsic light scattering in the sample significantly alters pump–probe measurements around the pump wavelengths (effective ΔA signal reaches –120 mOD at excitation energies of ~120 nJ), to suppress its influence on the transient kinetics we used dual chopping with synchronized mechanical choppers (MC1000, Thorlabs, and 3501, New Focus) installed in the pump and probe beams. The inset in Fig. 1 shows the timing sequence of pulses for this configuration. In the first position of the chopper blades when both beams are incident on the sample, the spectrometer measures the spectrum of the probe pulse, transmitted through the excited sample $E^*_{out}(\lambda)$ and mixed with the scattered pump pulse $S_{bR}(\lambda)$: $S_1(\lambda) = E^*_{\mathrm{out}}(\lambda) + S_{bR}(\lambda)$. In position 2 the pump beam is blocked, and the spectrometer measures the spectrum of the probe pulse transmitted through the nonexcited sample (reference spectrum) $S_2(\lambda) = E_{\mathrm{out}}(\lambda)$. In the third position the probe beam is blocked, and we measure only the spectrum of scattered pump, $S_3(\lambda) = S_{bR}(\lambda)$. In the fourth position, both beams are blocked by chopper blades so that only the dark background of the photodiode array is measured. The transient signal is then calculated as

$$\Delta A(\lambda) = -\log_{10}\left[\frac{(S_1(\lambda) - S_3(\lambda))}{S_2(\lambda)}\right]. \quad (1)$$

Treatment of 2D pump–probe data was performed using global analysis as described in Ref. 6 (see the Appendix therein).

The beam profiles in the focal plane were measured by scanning of a small pinhole and a razor blade (the "knife-edge" method) across the beams. The spatial distributions of the pump and probe beams correspond to Gaussian profiles with a confidence of $R = 0.993$; the FWHM of pump and probe beams are 43 ± 2.5 and 34 ± 2 μm, respectively. In this configuration, the saturation energy density of 4.8×10^{15} photons/cm^2 (Ref. 4) corresponds to the energy of $E_s = 25$ nJ. The instrument response function of the pump–probe setup was measured to be 35 fs FWHM using sum-frequency generation in a 100 μm thick β-barium borate crystal. The time and frequency resolved transient kinetics were measured using probe scans with nonequally distributed steps in a delay range up to 600 ps; the minimal step was 10 fs. The chirp and power scans were measured with a photodiode (PD3) at different delays after excitation (20, 40, and 300 ps) at different wavelengths using a set of a 10 nm bandwidth interference filters (Thorlabs, Edmund Optics). The excitation laser pulses were centered at 565 nm, nearby the absorption maximum of the light-adapted bR (Fig. 2). Their spectral width (~40 nm) and their TL duration (22 fs FWHM) were comparable to the excitation pulses used in Ref. 15. For measurements of nonlinear transmission, the photodiodes PD1 and PD2 measuring the pump pulse energy before and after the sample were calibrated using a power meter (Fieldmaster, Coherent). The short-term stability of the laser source (measured after the pulse shaper) was typically 0.3%; with long-term stability ~1%. In the chirp scans, the standard deviation of the differential absorption signal was typically ~0.1 mOD.

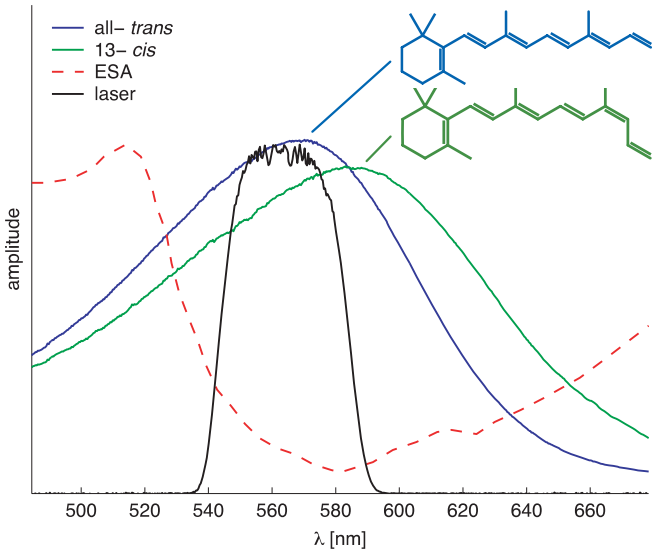

FIG. 2. Measured absorption spectrum of all-*trans* bR, its K-intermediate (13-*cis* isomer, see in Ref. 4 *SI* online), and excited-state absorption (ESA, adapted from Fig. 5 in Ref. 30) in comparison to the laser excitation spectrum.

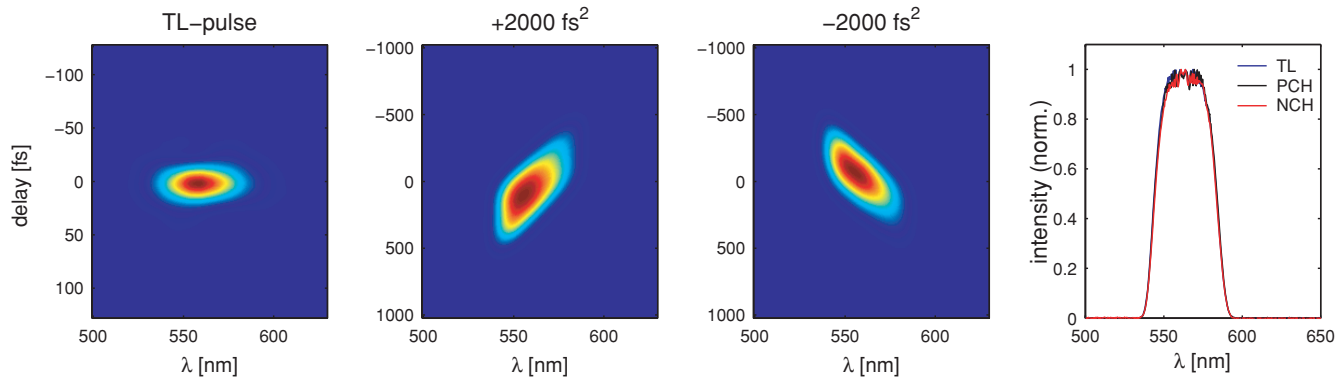

FIG. 3. FROG traces measured for the TL, PCH and NCH pulses (as indicated). The rightmost panel compares the spectra of the TL and chirped laser pulses.

B. Pulse characterization

The excitation pulses traveling from the noncollinear optical parametric amplifier to the pump–probe setup through an acousto-optic pulse shaper (the Dazzler, Fastlite) were measured using third-order frequency-resolved optical gating (FROG) (Ref. 20) in an apparatus described in Ref. 1. The FROG traces were analyzed using the commercial program FROG3 (Femtosoft Technologies). As an example, Fig. 3 shows the measured FROG traces for the TL, positively chirped $+2000$ fs^2 (PCH), and negatively chirped -2000 fs^2 (NCH) pulses. Chirping stretches the initial TL pulse with 22 fs FWHM duration up to ~400 fs FWHM for the NCH and PCH pulses. No significant distortions of the spectral shapes were observed by applying these modulations.

C. Sample preparation

For measurements, the light-adapted bR-sample with a typical optical density (OD) of 0.6–1 was circulated through a flow cell with 150 μm thick fused silica windows (see absorption spectrum in Fig. 2). The bR containing membranes from *Halobacterium salinarum* were prepared according to the procedure described in Ref. 4 and suspended in a buffer with a typical *p*H of 6.5. During measurements, the 3 ml reservoir containing the sample was kept in the light-adapted state by continuous illumination with a halogen lamp and held on ice. In the experiments we used cells with 0.4, 0.8, and 1 mm path lengths; no significant difference in the measured dependencies was detected. For the experiments reported in the paper, we used a 0.8 mm cell and OD ~1. We did not observe formation of any milky substance in the sample during or after experiments (typical duration of 4–5 h) as was reported in Ref. 15. However, a systematic lowering of *p*H by ~ 0.5 was observed after transient absorption measurements.

III. RESULTS AND DISCUSSION

The simplest coherent control scenario can be implemented by applying linear chirp to the excitation pulses, which is an appropriate benchmark for theoretical and experimental studies. Therefore, in this study for the investigation of the phase sensitivity of retinal isomerization in bR we used excitation pulses with different chirp magnitudes and signs. The chirp rate was varied in the frequency domain within [–2000, +2000] fs^2 using an acousto-optic shaper.

A. Chirp scans

The chirp dependence of the transient absorption signal $\Delta A = A^* - A_0$ was measured 40 ps after excitation at 630 nm which is close to the maximum of the transient differential absorption spectrum $\Delta A(\lambda)$ for the *trans* to *cis* photoreaction of interest, as used in our earlier studies, and thus carries direct information about the amount of 13-*cis* photoproduct [see Fig. 5(b) in Ref. 4]. In contrast, Florean *et al.*[15] used 650 nm as a monitoring wavelength, which is located at the maximum slope of the differential spectrum. We note that this choice of probe wavelength makes the experiment most sensitive to changes in the photoproducts produced, as opposed to maximizing the target photoproduct. In order to directly compare to the work of Florean *et al.*,[15] we also examined the dependence at 650 nm. At moderate excitations corresponding to the incident energies of 20–40 nJ ($3–7\times10^{15}$ photons/cm^2) and comparable to the saturation energy of the $S_0 - S_1$ retinal electronic transition (E_s ~ 25 nJ for the given optical layout, see in Sec. II) we are clearly observing ν-shaped chirp dependence [Figs. 4(a) and 4(b)] with a minimum about zero chirp (i.e., for the TL pulse). Increasing the excitation level changes the chirp dependence significantly. At an excitation energy of 126 nJ (~ 2.5×10^{16} photons/cm^2) the chirp dependence at 630 nm becomes only slightly asymmetric, but a ~ 20% increase of the transient absorption signal is observed at 650 nm for the TL pulse [Figs. 4(c) and 4(d)]. It should be noted that the chirp dependence measured at 650 nm at this excitation energy qualitatively agrees with the observations in Ref. 15 at similar excitation levels. However, due to inadequate precision realized in Ref. 15 (~5%), the authors were not able to resolve any chirp dependence at excitation energy of 21 nJ.[21]

Simultaneous measurement of the absorbed energy $\Delta E = E_{in} - E_{out}$ also clearly displays a significant chirp dependence, the shape of which does not change upon increase of the excitation level [Figs. 4(e) and 4(f)]. At all excitation energies used in the study, the amount of absorbed energy is maximal for TL pulses. The clearly resolved asymmetry in the chirp dependence of the transient signals at excitations

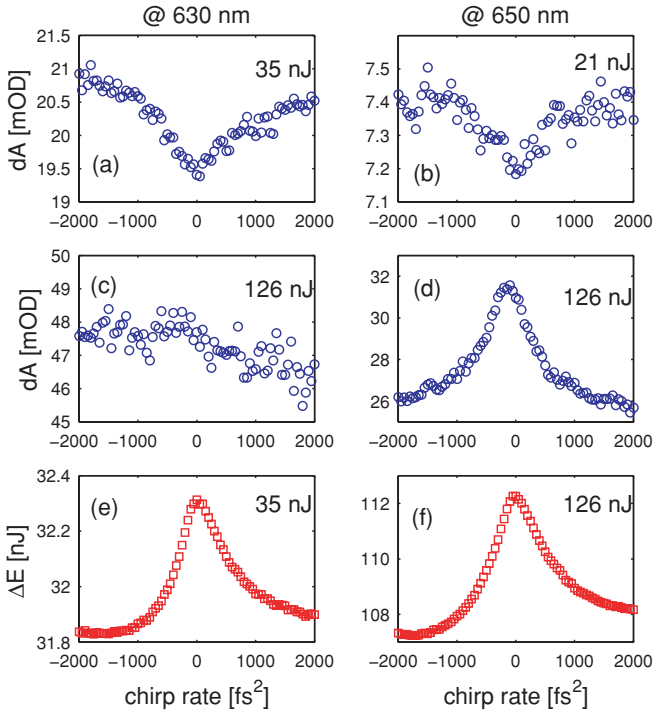

FIG. 4. Chirp dependence of induced absorption ΔA at different excitation energies (as indicated) probed at 630 nm (a, c) and 650 nm (b, d). Bottom panels e and f show the amount of excitation energy absorbed by bR as a function of chirp rate.

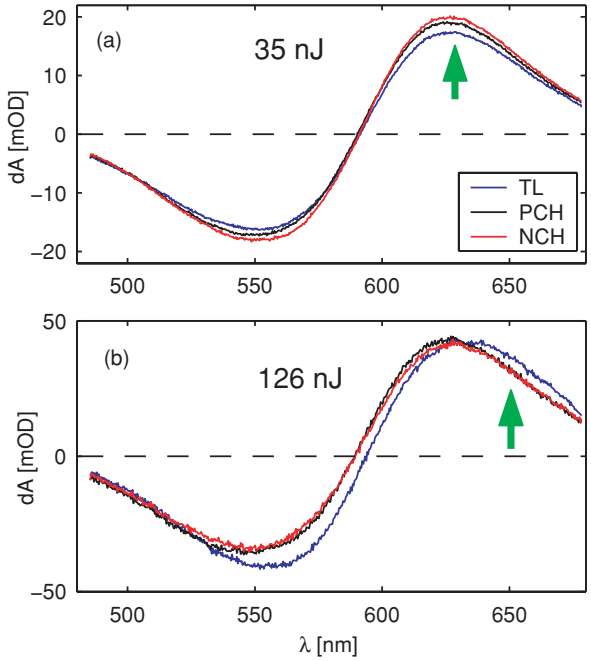

FIG. 5. Differential absorption spectra of bR measured at 40 ps delay after excitation with TL and chirped pulses (PCH +2000 fs^2, NCH −2000 fs^2) for excitation energies of 35 nJ (a) and 126 nJ (b). Arrows indicate wavelengths, where the chirp dependence was monitored (Fig. 4).

<40 nJ and in the absorbed energy unambiguously confirms the phase sensitivity of the primary steps in the isomerization of retinal in bR. If these effects were simply the result of an increase in pulse duration, the measured quantities in Fig. 4 would be symmetric about zero chirp.

B. Transient kinetics

To understand the controversial character of the chirp dependence and to characterize the isomerization kinetics of bR at high excitation levels driven by chirped pulses, we measured the time-resolved transient absorption spectra $\Delta A(\lambda, \tau)$ in a delay window $\tau = [-0.5, 600]$ ps. We found that they differ strongly for low and high excitation. At low and moderate excitations (<40 nJ) with chirped and TL pulses the ΔA spectra measured at 40 ps delay display identical shapes, similar to previous measurements,[4] but with well-resolved differences in their magnitudes [Fig. 5(a)]. The difference between TL and negatively chirped pulses reaches 16% and directly reflects a change in the isomerization efficiency due to variation of the chirp. The minimal magnitude of the ΔA spectrum and thus the minimal isomerization yield of the 13-*cis* isomer is observed for the TL pulse. This is in full agreement with the chirp scans performed at this excitation energy [Figs. 4(a) and 4(b)] and with theoretical predictions. It is notable that the NCH excitation pulse leads to higher magnitude of the ΔA spectrum (in agreement with the ΔA signal in the chirp scans), i.e., this pulse increases the isomerization efficiency slightly better as compared to the PCH pulse. The isomerization kinetics are not significantly affected by the shape of the excitation pulses at this excitation level — the corresponding time constants recovered from the global analysis of $\Delta A(\lambda, \tau)$ remain similar for all pulses and agree well with those previously reported in Ref. 6. Further increasing the delay time does not significantly change the shapes and magnitudes of the ΔA spectra. The decay-associated spectra (DAS) of the long-lived component are similar to spectra measured at 40 ps delay (Fig. 6, top row), from which we conclude that the formation of the 13-*cis* retinal isomer is almost complete at this delay.

Increasing the excitation energy drastically changes the photochemistry. Upon excitation with a TL pulse having 126 nJ energy (~200 GW/cm^2), the whole ΔA spectrum measured at 40 ps delay becomes redshifted by ~5 nm [Fig. 5(b)]. Thus, the 20% growth of the transient absorption signal around zero chirp observed at 650 nm [Fig. 4(d)] is due to this spectral shift and not the result of maximization of the 13-*cis* population as was stated in Ref. 15. This redshift remains for long delay times. Excitation with an intense TL pulse decreases the amplitude at the maximum in the ΔA spectrum [Fig. 5(b)], compared to excitation with chirped pulses; however, the signal at 560 nm (roughly proportional to the bleach of the all-*trans* isomer) is increased. A possible reason for this could be a photoinduced degradation of retinal upon excitation with high-energy pulses as found previously.[22–24] Therefore, we can conclude that the yield of retinal isomerization in bR lowers upon excitation with very intense TL pulses. It is important to note that the overall photoisomerization kinetics are also changed upon excitation with very intense pulses and at least one more DAS-component is required to satisfactorily describe the observed transient kinetics (Fig. 6, bottom row). For illustration, Fig. 7 displays the decay traces at 630 and 650 nm during the first 5 ps of isomerization upon excitation with differently chirped pulses having energies of 35 and

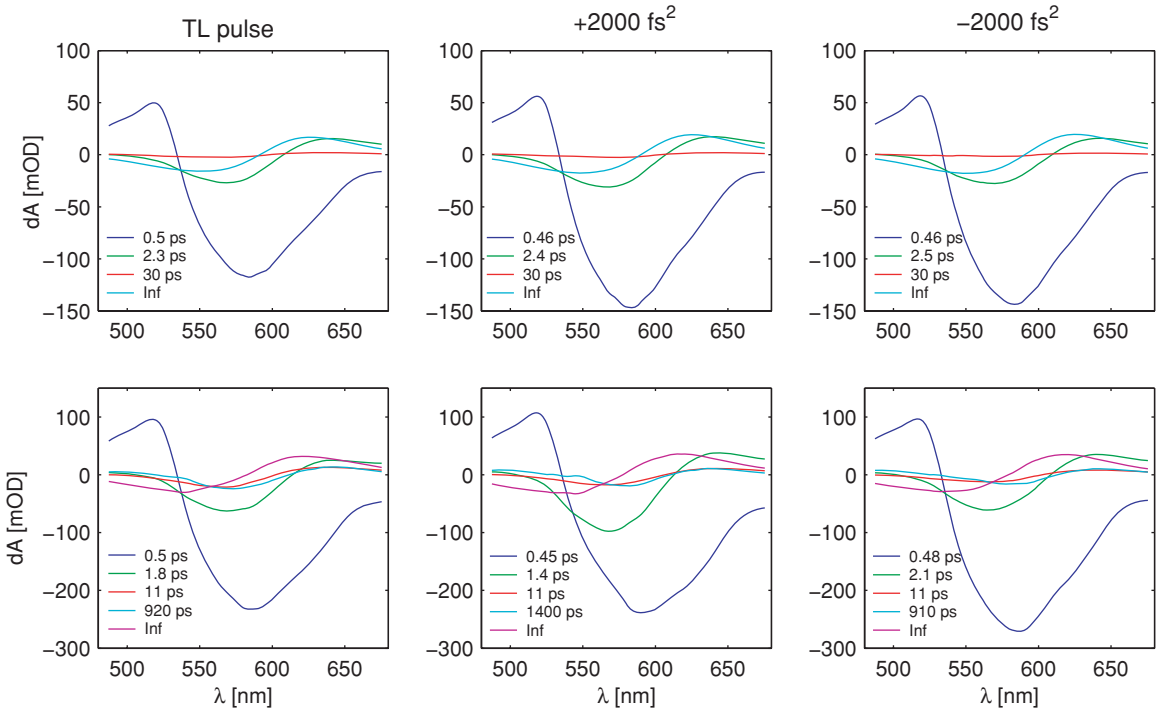

FIG. 6. Decay-associated spectra recovered from the transient kinetics driven by the TL, PCH (+2000 fs^2) and NCH (–2000 fs^2) excitation pulses having 35 nJ (top row) and 126 nJ (bottom row) excitation energies.

126 nJ. This modification in the kinetics is most apparent at 650 nm [Fig. 7(d)]. Chirping of the excitation pulse increases its duration (up to ∼400 fs for ± 2000 fs^2 chirp rates), leading to a broader instrument response function and thus to broadening of the measured signal around zero delays. This effect can be readily observed in Fig. 7 — the transient kinetic traces become broadened relative to the transform limited case. It should be noted that in Ref. 15 the authors also measured the first steps in isomerization kinetics using strongly chirped pulses (–35000 fs^2, which will stretch the TL pulses over a few ps); however, no broadening near zero delay was observed (see Fig. 5 therein). This allows us to suggest, as an additional complication, that the chirp calibration in Ref. 15 may have been inaccurate.

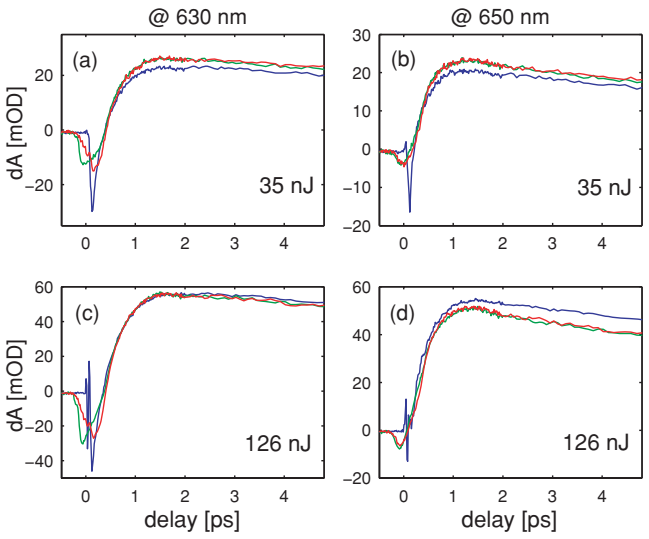

FIG. 7. Isomerization kinetics monitored at 630 and 650 nm during the first 5 ps after excitation with transform limited (blue), + 2000 fs^2 (green), and –2000 fs^2 (red) chirped pulses having 35 and 126 nJ energies.

C. Nature of the spectral shift

The presence of a spectral shift at long delays upon excitation with intense TL pulses does not allow a description of the observed isomerization kinetics within the framework of a two-component model (all-*trans* + 13-*cis* isomers); it requires the inclusion of at least one (or more) additional photoproduct(s). It could be, e.g., the absorption of a solvated electron produced in bR due to ionization of the protein. It is known that the optical absorption of solvated electrons has a maximum around 700–720 nm in water[25] and in water-containing micelles[26,27] where it persists tens of ns[27,28] and much longer in biological molecules.[29] Upon excitation with visible light the ionization of a protein (or the surrounding water) is possible only due to multiphoton processes and thus should have a strong nonlinear behavior. To check this, we measured the chirp dependence of the transient absorption signal at 600 nm (see Fig. 8), where it is very sensitive to the spectral shift but does not overlap with the laser spectrum. Chirping of the excitation pulses leads to temporal stretching and thus changes the instantaneous pulse intensity. The sample was diluted to OD 0.2 to reduce the influence of the demonstrated intrinsic phase sensitivity of retinal isomerization and to make the distribution of the electric field more uniform along the cell. Indeed, a very sharp hole is observed

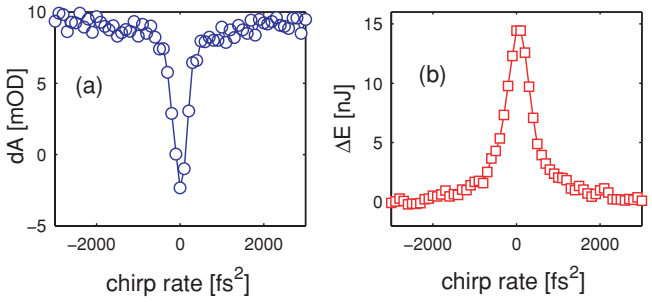

FIG. 8. Chirp dependence of induced absorption monitored in diluted bR at 600 nm (a) and energy absorbed in pure buffer (b) upon excitation with the 160 nJ pulses.

around zero chirp, where the signal changes from +8 to –4 mOD within 500 fs^2 [Fig. 8(a)], which is much faster and stronger than in the chirp dependence measured at 650 nm at similar excitations [Fig. 4(d)]. Note that in this experiment the spectrum of the excitation pulse was narrowed to get 25 fs TL pulses; the 500 fs^2 chirp rate stretches its duration to ~110 fs so that an instantaneous strength of the corresponding electric field changes only by a factor of ~2. It is also notable that the sign of the induced ΔA signal changes from positive (darkening) to negative (bleaching). This sign change can only occur due to very a strong spectral shift (cf. Fig. 5). The extent of the highly nonlinear multiphoton process can be tested by doing the control experiment without protein present. However, this control was not done in Ref. 15. The measured absorbed energy of the excitation light pulses in pure buffer [Fig. 8(b)] also exhibits a strong peak at zero chirp (i.e., for the TL pulse) indicating strong absorption at highest intensities (~200 GW/cm^2). At this intensity level up to 10% of the incoming light is absorbed through nonresonant multiphoton processes leading to ionization (note that the generation of the white-light was not observed). Under resonant conditions, the multiphoton absorption process is amplified by orders of magnitude and would also lead to ionization of bR and creation of solvated electrons that have a broad spectrum to the red of that of the *cis* photoproduct. These observations lead us to conclude that the origin of the observed spectral shift is the absorption of solvated electrons produced by the ionization of bR and other possible photoproducts formed as a consequence. The key point is that the spectral marker used in the the Florean *et al.* study[15] reports on photoproducts other than simply the 13-*cis* bR isomer.

D. Power dependence and role of the ESA

We investigated the phase response of the retinal isomerization in a wide range of excitation energies; Figs. 4 and 7 illustrate only two points in this dependence (35 and 126 nJ). Figure 9(a) shows the power dependence of the relative isomerization yield, defined as $IY = \Delta A(630)/\Delta E$, for different pulses measured in a range of 8–160 nJ excitation energies. Even at the lowest energies used in this study (8–15 nJ) the influence of chirp on the isomerization yield is still clearly present. The maximal effect of pulse shaping is observed at excitation energies of 30–50 nJ; any further increase of the pulse energy decreases the difference in the above de-

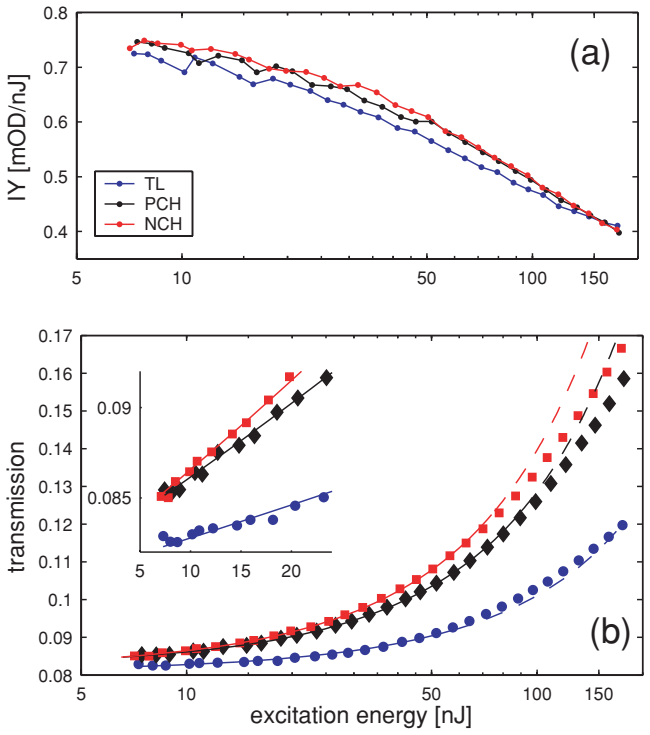

FIG. 9. Power dependence of the relative isomerization yield IY (a) and transmission of bR (b) measured with TL and chirped pulses (PCH +2000 fs^2, NCH −2000 fs^2). Solid-dashed lines in (b) correspond to fits to the data using a two-level model (see text).

fined yield due to the influence of the spectral shift. The general monotonic decrease of the isomerization yield at excitations > 50 nJ is most likely due to nonradiative loss of the excitation through transfer from the excited state S_1 to higher states $S_{2..n}$ via ESA. While the $S_1 - S_2$ absorption cross section is relatively small in the pump spectral region (minimum at 585 nm;[30] see Fig. 2), very strong excitation that saturates the $S_0 - S_1$ absorption channel will highly populate the S_1 state. This would allow for significant transfer of population to S_2, especially considering its long lifetime (0.75 ps according to Ref. 31). This effect would be more pronounced for chirped pulses since, due to the increased pulse duration, this S_1 population has a longer temporal interaction with the laser field to accumulate population in S_2. However, the fact that an increase in excitation energy leads to a lowering of the isomerization yield [Fig. 9(a)] suggests that the contribution to formation of *cis*-isomers starting from $S_{2..n}$ excited states is in fact not significant.

The coherent character of the isomerization control manifests itself as the asymmetry in the chirp dependence of the transient absorption signals and the absorbed energy ΔE (Fig. 4). This asymmetry is also observed in the power dependence of the isomerization yield at moderate excitation energies [Fig. 9(a)]; however, it is much better resolved in the transmission dependence since the accuracy of such measurements is much higher [Fig. 9(b)]. The difference in transmission measured with the NCH and PCH pulses is present over the whole excitation range. At the smallest energies the difference in transmission measured with TL and chirped pulses is also clearly resolved [see inset in Fig. 9(b)]. Up to excitations of ~60 nJ this dependence can be formally fit to theoretical

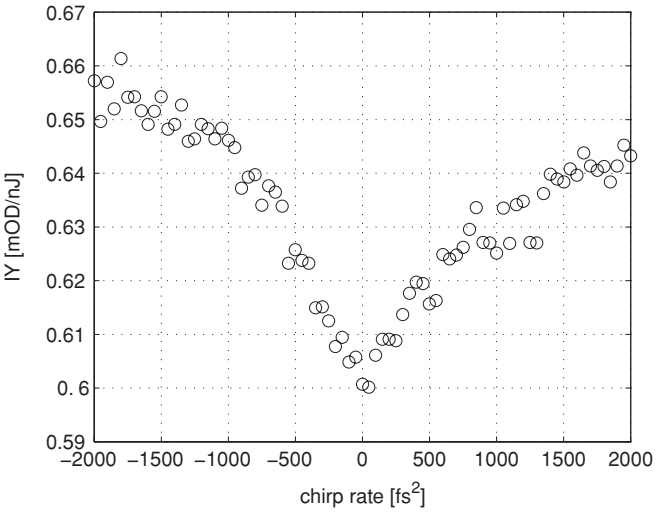

FIG. 10. Chirp dependence of the isomerization yield *IY* at an excitation level of 35 nJ.

expressions describing nonlinear transmission of a two-level system for a thick optical layer in the stationary and nonstationary approximations:[32,33]

$$\frac{I}{I_s} = \frac{1}{(1-T)} \log\left(\frac{T}{T_0}\right), \tag{2}$$

$$T = \frac{E}{E_s} \log[1 + T_0(e^{E/E_s} - 1)], \tag{3}$$

where $I_s = 1/\sigma_e\tau$ ($E_s = 1/\sigma_e$) is the saturation intensity (energy) of the $S_0 - S_1$ electronic transition, σ_e is the effective absorption cross section, τ is the relaxation time of the excited level, and T_0 is the linear transmission. The nonstationary approach holds for excitation with the TL pulse since its duration is much shorter than the relaxation of the retinal excited state (22 versus 450 fs), whereas for the PCH and NCH pulses whose durations are ~400 fs, the stationary approach is a more relevant approximation. Calculated theoretical dependencies are shown in Fig. 9(b) by solid-dashed lines; they coincide with experimental data with a confidence of $R = 0.99$ for excitation levels <60–80 nJ (solid lines). At excitations higher than 80 nJ the deviations between calculated (dashed lines) and measured dependence are caused by the influence of the ESA (note that the spectral shift observed in the transient absorption spectra is irrelevant in the measurement of the transmission). The presence of ESA affects also the power dependence at low excitations. Even if the S_2 state is not populated, the magnitude of the effective absorption cross section recovered from fitting becomes several times smaller as compared to those calculated from the absorption spectrum of bR.[34] For high excitations, the formal fit in the stationary case can be significantly improved using a three-level model,[35] which directly takes into account the saturation effects caused by ESA. However, for moderate excitations ≤60 nJ where the isomerization yield can be controlled by up to 16% using chirped pulses, the contribution of ESA is unimportant.

E. The control mechanism

On the basis of our experimental observations, we can suggest two competitive physical effects controlling the isomerization efficiency at excitations lower than the ionization threshold: control of the population transfer via the pump-dump scenario[11] and intrinsic control of the isomerization efficiency via focusing and passing of an accelerated wave packet through the conical intersection, the wave packet acceleration (WPA) scenario. The first mechanism requires a positive chirp in the excitation pulses in order to keep the wave packet far away from the bottom of the excited state surface and, thus, to prevent a lowering of the excited-state population due to stimulated emission. Thus, the chirp dependence of the isomerization yield should be asymmetric: more photoproduct for the PCH and less for the NCH pulses. However, in open quantum systems the difference in the populations excited with the NCH and PCH pulses is small[13] and almost vanishes in the presence of the ESA;[12] the chirp dependence of the induced population becomes a nearly symmetric ν-shape of which the minimum corresponds to the TL pulse. Also, increasing the system–bath interaction strength sufficiently decreases the overall population control.[13] Taking into account the strong dephasing of the electronic transition in retinal (~13 fs according to Ref. 36) and fast isomerization dynamics (formation of J-intermediate occurs within ~450 fs, Ref. 6) it becomes clear why the overall control magnitude is only 16% even at excitation energies approximating the saturation energy.

The second mechanism can be understood by consideration of the wave packet propagation through the conical intersection in the framework of a semiclassical model proposed in Ref. 37. The authors describe isomerization as a scattering of the wave packet at the conical intersection, considering the seam as an effective aperture of which the "size" depends on the wave packet speed, i.e., the efficiency of isomerization is affected by the chirp of the excitation pulses. However, unlike the enhancement of population transfer, this mechanism requires a negative chirp in the excitation pulses ("blue" leading edge and "red" trailing edge), which accelerates the downhill movement of the wave packets toward the conical intersection. Thus, the chirp dependence should again be asymmetric with respect to the chirp sign, but in the opposite direction to the pump-dump mechanism. Mixed together, pump-dump and WPA controls will result in the isomerization chirp dependence with an asymmetric ν-shape having higher efficiency for the negatively chirped pulses, as is observed in the experiment at moderate excitation energies [Fig. 4(a)]. This asymmetry becomes more apparent in the chirp dependence of the *IY*, i.e., after normalization of the induced absorption change ΔA to absorbed energy ΔE (Fig. 10). Note that the authors of Ref. 37 did not emphasize the power dependence of this intrinsic isomerization control (WPA) and did not include damping effects due to interaction with the bath; however, from the numerical simulations performed in Ref. 7 it follows that this control also works in the weak-field limit. Ideally, the most effective control of the isomerization efficiency can be reached through the use of both positive and negative chirps, and this is exactly what has

been observed in structures of optimal pulses obtained in the weak-field experiment.[4] The Wigner plot of the pulse structure reveals positively chirped blue and negatively chirped red components of the spectrum.[38]

Note that to support their experimental findings, Florean *et al.*[15] refer to the theoretical paper of Hoki and Brumer[39] in which a numerical simulation of optimal control of photoisomerization was performed. In this work, an unusual target was used for numerical optimization of the photoisomerization, that of the ratio of the photoproduct population to the pulse area of the excitation field. The authors found that the pulse of highest intensity and shortest duration maximizes the population of photoproduct. However, the amount of a photoproduct generated in a photoreaction should always be defined with respect to absorbed light energy, which gives the yield of a photoreaction. While the pulse area A_p is roughly proportional to the product of pulse duration τ_p and the magnitude of the electric field ε_f, i.e., $A_p \propto \tau_p \varepsilon_f$, the energy of the pulse E is proportional to the product of pulse duration and squared field amplitude: $E \propto \tau_p \varepsilon_f^2$. Therefore, by increasing the pulse duration, e.g., ten times and keeping the pulse area at a constant level, the pulse energy will proportionally decrease ten times. In this theoretical work, the optimal pulse has roughly ten times more energy than the "anti-optimal" and consequently the amount of photoproduct (*cis*-population in the paper) is much higher (as can be seen by inspection of Figs. 1 and 2 in Ref. 39). From an experimental standpoint, such control as calculated in Ref. 39 can be achieved by simply increasing or reducing the laser power. This theory does not support the experimental observations as suggested in Ref. 15. Experimentally, the isomerization yield is a more relevant optimization target, rather than the absolute population of the product state not linked to the absorbed or incident excitation energy.

IV. CONCLUSIONS

We experimentally demonstrated the coherent control of the all-*trans* to 13-*cis* isomerization of retinal in bacteriorhodopsin in the high intensity regime. The isomerization efficiency is minimized by excitation with transform limited pulses and increases by up to 16% upon excitation with chirped pulses if the excitation level does not exceed an intensity of $\sim$100 GW/cm^2. Above this level isomerization becomes distorted, most likely due to multiphoton ionization of the protein and generation of solvated electrons, and potentially other photoproducts. This results in a red shift of the transient absorption spectra, which explains a growth of transient signal at 650 nm observed in Ref. 15 and in the present work using high intensity TL pulses. Asymmetry in the chirp dependence of the absorbed energy and isomerization efficiency is direct evidence of the coherent nature of the control over isomerization. Such features in the isomerization control can be qualitatively explained in the frameworks of the pump-dump and wave packet focusing/acceleration mechanisms.[7,11,37] Control of isomerization is observed in a wide range of excitation energies; the lowest excitation levels link this experiment to the weak-field study performed earlier.[4] From the theoretical work of Katz *et al.*[7] it follows that the degree of control depends on the system–bath coupling strength (see inset in Fig. 4 therein). Recent investigations of the system–bath interaction in a solvated dye by means of coherently controlled 2D-spectroscopy demonstrated that this coupling can be effectively controlled using not only phase shaping, but mainly amplitude shaping of excitation pulses.[40] In this regard, it becomes clear why the degree of control in the weak-field experiment[4] was higher than in the experiments reported here.

In contrast to the work of Florean *et al.*,[15] our experimental results and their analysis lead us to conclude that the quantum coherence does play a significant role in the control of retinal isomerization even at high excitation. The fact that we observe enhanced isomerization yields that are phase dependent up to fairly high intensity indirectly illustrates how highly optimized the reaction coordinate in bR is. For the chirped pulses, the peak power is lower and there is a greater degree of involvement of the first excited state surface, than in the indiscriminate multiphoton absorption to higher electronic states as would be the case for transform limited pulses. The involvement of the first excited state appears to dominate up until the peak power is high enough to significantly ionize the protein or other unrelated reaction channels at which point it becomes difficult to separate isomerization from other photoproducts. Multiphoton absorption places the system significantly higher above the barrier to isomerization than the natural process involving the first excited state. However, from our findings, it is now clear that the reaction rate is independent of excess energy above the barrier, otherwise higher peak power and multiphoton processes would show higher isomerization yields in this nonlinear regime. The functional response of bR is effectively barrierless. The branching ratio of isomerization to nonradiative relaxation back to the ground state depends critically on the dynamics and transmission probability for motion through the conical intersection separating the *trans* and *cis* potential energy surfaces. The present observations are understandable as the system is already moving near theoretical limits for sampling the conical intersection. The reaction coordinate is highly directed. In this respect, the problem of multiphoton absorption and generation of unrelated photoproducts, as identified in this work, is likely going to be an even more serious problem for coherent control studies of complex molecules with less robust excited state reaction dynamics than bR. The present work illustrates the importance of characterizing the coherent control of molecular photochemistry at low intensity, ideally in the weak-field limit, to isolate mechanistic details and aspects of quantum coherence on the reaction coordinate of interest.

ACKNOWLEDGMENTS

The experiments were performed at the Chemistry Department of the University of Toronto, Canada. The research was supported by the Natural Sciences and Engineering Research of Canada. V.I.P. and R.J.D.M. acknowledge support through the Max Planck Society.

[1] V. I. Prokhorenko, A. M. Nagy, and R. J. D. Miller, J. Chem. Phys. **122**, 184502 (2005).
[2] J. Hauer, T. Buckup, and M. Motzkus, J. Chem. Phys. **125**, 061101 (2006).

[3]P. van der Walle, M. T. W. Milder, L. Kuipers, and J. L. Herek, Proc. Natl. Acad. Sci. U.S.A. **106**, 7714 (2009).
[4]V. I. Prokhorenko, A. M. Nagy, S. A. Waschuk, L. S. Brown, R. R. Birge, and R. J. D. Miller, Science **313**, 1257 (2006).
[5]J. K. Lanyi, Biochim. Biophys. Acta **1757**, 1012 (2006).
[6]V. I. Prokhorenko, A. M. Nagy, L. S. Brown, and R. J. D. Miller, Chem. Phys. **341**, 296 (2007).
[7]G. Katz, M. A. Ratner, and R. Kosloff, New J. Phys. **12**, 015003 (2010).
[8]G. Cerullo, C. J. Bardeen, Q. Wang, and C. V. Shank, Chem. Phys. Lett. **262**, 362 (1996).
[9]C. J. Bardeen, V. V. Yakovlev, J. A. Squier, and K. R. Wilson, J. Am. Chem. Soc. **120**, 13023 (1998).
[10]O. Nahmias, O. Bismuth, O. Shoshana, and S. Ruhman, J. Phys. Chem. A **83**, 5013 (2005).
[11]D. J. Tannor and S. A. Rice, J. Chem. Phys. **83**, 5013 (1985).
[12]B. D. Fainberg and V. A. Gorbunov, J. Phys. Chem. A **111**, 9560 (2007).
[13]D. Gelman and R. Kosloff, J. Chem. Phys. **123**, 234506 (2005).
[14]M. Greenfield, S. D. McGrane, and D. S. Moore, J. Phys. Chem. A **113**, 2333 (2009).
[15]A. C. Florean, D. Cardoza, J. L. White, J. K. Lanyi, R. J. Sension, and P. H. Bucksbaum, Proc. Natl. Acad. Sci. U.S.A. **106**, 10896 (2009).
[16]K. A. Freedman and R. S. Becker, J. Am. Chem. Soc. **108**, 1245 (1986).
[17]Y. Koyama, K. Kubo, M. Komori, H. Yasuda, and Y. Mukai, Photochem. Photobiol. **54**, 433 (1991).
[18]J. Tittor and D. Oesterhelt, FEBS Lett. **263**, 269 (1990).
[19]S. L. Logunov and M. A. El-Sayed, J. Phys. Chem. B **101**, 6629 (1997).
[20]R. Trebino, K. W. DeLong, D. N. Fittinghoff, J. N. Sweetser, M. A. Krumbügel, B. A. Richman, and D. J. Kane, Rev. Sci. Instrum. **68**, 3277 (1997).
[21]This value of 21 nJ incident energy corresponds to 12 nJ in Ref. 15 defined as "entering the region of the cell where the pump and probe pulse overlap" with bR having OD 1. We report incident pulse energy, as under highly nonlinear conditions it is not possible to use linear extrapolation to estimate pulse energies within a sample cell.
[22]R. Govindjee, S. P. Balashov, and T. G. Ebrey, Biophys. J. **58**, 597 (1990).
[23]J. Czégé and L. Reinisch, Photochem. Photobiol. **53**, 659 (1991).
[24]M. B. Masthay, D. M. Sammeth, M. C. Helvenston, C. B. Buckman, W. Y. Li, M. J. Cde-Baca, and J. T. Kofron, J. Am. Chem. Soc. **124**, 3418 (2002).
[25]E. J. Hart and M. Anbar, *The Hydrated Electron* (Wiley, New York, 1970).
[26]V. Calvoperez, G. S. Beddard, and J. H. Fendler, J. Phys. Chem. **85**, 2316 (1981).
[27]J. L. Gebicki, L. Gebicka, and J. Kroh, J. Chem. Soc., Faraday Trans. **90**, 3411 (1994).
[28]Y. J. Lee, T. W. Kee, T. Q. Zhang, and P. Barbara, J. Phys. Chem. B **108**, 3474 (2004).
[29]R. Katoh, J. Photochem. Photobiol. A **189**, 211 (2007).
[30]K. C. Hasson, F. Gai, and P. A. Anfinrud, Proc. Natl. Acad. Sci. U.S.A. **93**, 15124 (1996).
[31]F. Gai, K. C. Hasson, J. C. McDonald, and P. A. Anfinrud, Science **279**, 1886 (1998).
[32]V. I. Prokhorenko, M. V. Melishchuk, and E. A. Tikhonov, Zh. Tekh. Fiz. **51**, 955 (1981).
[33]V. I. Prokhorenko, M. V. Melishchuk, and E. A. Tikhonov, Zh. Tekh. Fiz. **51**, 2603 (1981).
[34]For a two-level system {1,2} the absorption coefficient of a thin optical layer is $k = \sigma_{12}n_1 - \sigma_{21}n_2$, which results in power dependence either as $k(I) = k_0(1 + I/I_s)^{-1}$ (stationary regime) or $k(E) = k_0 e^{-E/E_s}$ (nonstationary regime of interaction) where I_s and E_s are defined over the effective absorption cross section $\sigma_e = \sigma_{12} + \sigma_{21}$ (see in text). For three-level system {1, 2, 3}, if population of third level is negligibly small, $k = \sigma_{12}n_1 - \sigma_{21}n_2 + \sigma_{23}n_2$. At low excitations, the power dependence of absorption coefficient can also be approximated by the equations given above, but I_s and E_s will be defined via $\sigma_e^{'} = \sigma_e - \sigma_{23}$.
[35]V. I. Prokhorenko, M. V. Melishchuk, and E. A. Tikhonov, Ukr. Fiz. Zh. **30**, 1480 (1985).
[36]A. Yabushita and T. Kobayashi, Biophys. J. **96**, 1447 (2009).
[37]A. Piryatinski, M. Stepanov, S. Tretiak, and V. Chernyak, Phys. Rev. Lett. **95**, 223001 (2005).
[38]A. Nagy, V. Prokhorenko, and R. J. D. Miller, Curr. Opin. Struct. Biol. **16**, 654 (2006).
[39]K. Hoki and P. Brumer, Phys. Rev. Lett. **95**, 168305 (2005).
[40]V. I. Prokhorenko, A. Halpin, and R. J. D. Miller, Opt. Express **17**, 9764 (2009).